JCTC Journal of Chemical Theory and Computation

Additive and Classical Drude Polarizable Force Fields for Linear and Cyclic Ethers

Igor Vorobyov,[†] Victor M. Anisimov,[†] Shannon Greene,[†] Richard M. Venable,[‡] Adam Moser,[‡,§] Richard W. Pastor,[‡] and Alexander D. MacKerell, Jr.*[,†]

Department of Pharmaceutical Sciences, School of Pharmacy, University of Maryland, Baltimore, Maryland 21201, and Laboratory of Computational Biology, National Heart, Lung, and Blood Institute, National Institutes of Health, Bethesda, Maryland 20892

Received November 30, 2006

Abstract: Empirical force field parameters consistent with the CHARMM additive and classical Drude based polarizable force fields are presented for linear and cyclic ethers. Initiation of the optimization process involved validation of the aliphatic parameters based on linear alkanes and cyclic alkanes. Results showed the transfer to cyclohexane to yield satisfactory agreement with target data; however, in the case of cyclopentane direct transfer of the Lennard-Jones parameters was not sufficient due to ring strain, requiring additional optimization of these parameters for this molecule. Parameters for the ethers were then developed starting with the available aliphatic parameters, with the nonbond parameters for the oxygens optimized to reproduce both gas- and condensed-phase properties. Nonbond parameters for the polarizable model include the use of an anisotropic electrostatic model on the oxygens. Parameter optimization emphasized the development of transferable parameters between the ethers of a given class. The ether models are shown to be in satisfactory agreement with both pure solvent and aqueous solvation properties, and the resulting parameters are transferable to test molecules. The presented force field will allow for simulation studies of ethers in condensed phase and provides a basis for ongoing developments in both additive and polarizable force fields for biological molecules.

1. Introduction

The ether moiety is an important functional group in molecules of biological and industrial importance. For instance, tetrahydrofuran (THF) is a model for ribose, deoxyribose, fructose, and other furanoses, and tetrahydropyran (THP) is a model for glucose and other pyranoses. Therefore, accurate parametrization of THF and THP is necessary for the development of both nucleic acid and carbohydrate force fields. Concerning linear ethers, dimethyl ether (DME), diethyl ether (DEE), and dimethoyxethane (DMOE) are commonly used organic solvents that are often utilized in a biological context, an example being the use of polyethylene glycol for the stabilization of protein based drugs for which DMOE is an ideal model compound.

From the physical chemical point of view ethers include a combination of the nonpolar aliphatic groups and polar oxygen atoms capable of participating in hydrogen bonds, including strong electrostatic interactions with cations. However, beyond that local hydrogen-bonding capacity, ethers are still relatively nonpolar, as evidenced by their small dipole moments and dielectric constants (e.g., the dipole moment of DEE is 1.15 and the dielectric constant is 4.24),[1] which has led to their use as solvents for organic synthesis. Therefore, the development of an empirical force field for this class of compounds requires attaining the right balance

* Corresponding author phone: (410)706-7442; fax: (410)706-5017; e-mail: amackere@rx.umaryland.edu. Corresponding author address: 20 Penn Street, Baltimore, MD 21201.

[†] University of Maryland.

[‡] National Institutes of Health.

[§] Current address: Department of Chemistry, University of Minnesota, 207 Pleasant St SE, Minneapolis, MN 55455.

10.1021/ct600350s CCC: $37.00
Published on Web 03/06/2007

of dispersion, electrostatic and repulsive forces governing the structure and dynamics of ethers in condensed phases and, thus, correctly describing a wide range of their properties. Facilitating such parameter development is the wide range of experimental data on the ethers. This includes a variety of data on the pure solvents[1] as well as free energies of solvation.[2] The availability of such data allows for an adequate training set of compounds to rigorously optimize the model as well as test compounds to validate the force field.

To date several empirical force fields for ethers have been presented. Linear ether (dimethyl ether (DME), methyl ethyl ether (MEE), DEE) parameters were developed as part of the MMFF94 force field.[3] Recently, parameters for both linear and cyclic ethers were developed in the framework of the MM4 force field of Allinger and co-workers.[4−8] Both MMFF94 and MM4 force fields provide accurate descriptions of the gas-phase properties of ethers including equilibrium geometries, vibrational frequencies, and torsional barriers. However, neither MM4 nor MMFF94 force fields were tested in condensed-phase simulations.

Emphasis on the reproduction of condensed-phase properties was placed in the development of the alkyl ether parameters determined in the framework of OPLS united atom (OPLS-UA)[9] and all-atom models (OPLS-AA).[10] In addition, OPLS parameters for THF were developed for the simulation of short polypeptides in this solvent.[11] In other work all-atom additive THF parameters were developed for use in MD simulations using an automatic optimization approach based on the simplex algorithm.[12,13] Ether parameters have also been developed for AMBER united-atom and all-atom force fields[14−16] and were tested using the compounds THF, dimethyl ether, and methyl ethyl ether model compounds.

Smith and co-workers have developed both additive and polarizable models of polyethylene oxide (PEO), its oligomers, and related compounds including DMOE. These efforts emphasized understanding the structure−property relationship in polymer electrolytes comprised of a PEO-based matrix, which was dopped with lithium salts.[17−23] The developed force field parameters for linear ethers were tested against a wide range of experimental structural, dynamic, and thermodynamic condensed-phase properties.

In this work we present a force field for both linear and cyclic ethers in the context of the CHARMM empirical force fields. Both an additive model and a polarizable model, based on a classical Drude oscillator, are considered. Motivation for the proposed work includes efforts in our laboratory to develop an additive force field for carbohydrates compatible with the CHARMM all-atom additive biomolecular force fields.[24−27] In addition, efforts are ongoing toward the development of a polarizable force fields for biomolecules based on a classical Drude oscillator. Those efforts have included the development parameters for water,[28,29] ethanol, alkanes,[30] and aromatics[31] along with the development of a general protocol for determination of the partial atomic charges and polarizabilities which was used to generate a preliminary polarizable force field for DNA.[32] More recently, an atom based anisotropic polarizable model has been developed,[33] which is applied in the proposed work.

2. Computational Methods

QM calculations were performed using the Gaussian 03 program suite.[34] Geometry optimizations were performed at the MP2(fc)/6-31G(d) level. The MP2/6-31G(d) level of theory has been found to provide molecular geometries consistent with gas-phase experimental data.[35] MP2/cc-pVTZ single-point energy calculations were performed on MP2/6-31G(d) optimized structures to obtain accurate estimates of molecular dipole moments, relative conformational energies, and torsional energy profiles. It was recently determined[36,37] that MP2/cc-pVTZ//MP2/6-31G(d) and MP2/cc-pVTZ//MP2-cc-pVTZ relative energies are quite similar for a number of small model compounds including alcohols and THP, motivating the use of the more economical hybrid method.

QM calculations on the complexes of model compounds with rare gas atoms (He and Ne) were performed at the MP3/6-311++G(3d,3p) level[38] with the intramolecular geometries fixed at the MP2/6-31G(d) optimized structures. The location of the minima were obtained using two distance scans based on MP3/6-311++G(3d,3p) single point energy calculations. The scans involved a preliminary 0.1 Å scan to identify the region of the energy minimum followed by a 0.01 Å scan from which the minimum was identified.

QM calculations on the complexes of model compounds with water molecule were performed using the gas-phase MP2/6-31G(d) optimized conformers of the model compound and the gas-phase experimental geometry of water molecule (R(OH) = 0.9572 Å, ∠HOH = 104.52°). For the additive CHARMM force field, constrained HF/6-31G(d) optimization of the complexes was performed where both monomer geometry and orientation were fixed, and only the interaction distance was optimized, as previously performed.[27,39] The optimized interaction distance and energy scaled by a factor of 1.16 were used as reference values for consistency with the CHARMM22 parameter development protocol.[27] The same protocol was applied for the polarizable model with MP2/6-31G(d) used to identify the water-model compound interaction minima with the interaction energies obtained via LMP2/cc-pVQZ(-g) single point calculations using the program Jaguar.[40] This level of theory provides an accurate estimate of the gas-phase interaction energies and geometries for a number of hydrogen-bonded dimers[41] at a reasonably low computational cost due to the use of the local MP2 (LMP2) method,[42,43] where only a subset of the virtual orbitals is used for the calculation of the perturbed wavefunction.

To obtain experimental target data for bond, valence angle, and dihedral angle distributions for the model compounds, surveys of the Cambridge Structural Database[44] were performed. Each model compound was used as a search template with acyclic R (i.e., R = C or H) substituent(s) allowed. Distorted structures, structures containing errors, ones with R-factor > 0.1, and powder structures were excluded from the surveys. Organometallic compounds and structures containing ions were also excluded, since the close proximity of ions and/or metals can substantially influence values of internal parameters. The histograms for the geometric parameter distribution were plotted using the program Vista.[45]

Their most probable values were obtained as the average of the values contributing to the largest peak on the histogram.

Empirical force field calculations were performed with the program CHARMM.[46,47] Polarizability was introduced using the classical Drude oscillator model by attaching massless charged particles to the core of polarizable atoms (e.g., only non-hydrogen atoms in the present model) via a harmonic spring with a force constant, k_D. The partial atomic charge of a polarizable atom q is redistributed between the Drude particle and atomic core. The sign of the charges on Drude particles q_D is chosen to be negative by analogy with the electron charge.[32] The magnitudes of q_D can be unambiguously determined from the atomic polarizabilities using the relationship $\alpha = q_D^2/k_D$. The charge on the atomic core q_c is determined by subtracting the Drude charge from the charge on the atom-Drude pair q, such that each atom-Drude pair forms a dipole $q_D \cdot d$ where d is the displacement vector going from the atomic core to its Drude particle. Thus, the electrostatic energy term U_{elec} in the additive potential energy function was modified to include Coulombic interactions between atomic cores and Drude particles. As in the additive CHARMM force field, interactions between core atomic charges q_c are excluded for 1−2 and 1−3 atom pairs. However, the U_{elec} term is modified to take into account screened 1−2 and 1−3 dipole interactions between Drude oscillators.[48] The screening is implemented through the smearing of the charge on the Drude particle and real atom using a Slater distribution with a dimensionless parameter 2.6.

In addition to the modified electrostatic term, the term U_{self} describing the self-energy of a polarizable atom via the harmonic term $0.5d\mathbf{K}^{(D)}d$ is included in the potential energy function.[32] The Drude force constant is generally treated as isotropic; however, for hydrogen bond acceptor atoms it is treated as a tensor $\mathbf{K}^{(D)}$, where the diagonal elements $K_{xx}^{(D)}$, $K_{yy}^{(D)}$, and $K_{zz}^{(D)}$ determine the stiffness of the atom-Drude bond in three orthogonal directions (defined using a local intramolecular reference frame) allowing for anisotropic polarizability; note that the higher values of K correspond to lower polarizability along a given direction. The case of $K_{xx}^{(D)} = K_{yy}^{(D)} = K_{zz}^{(D)} = k_D$ corresponds to the isotropic polarizability and is applied to all the carbon atoms in the present study. For oxygen the atomic polarizability anisotropy was defined as $K_{xx}^{(D)} = 1100$, $K_{yy}^{(D)} = 800$, and $K_{zz}^{(D)} = 1100$ kcal/(mol·Å^2) as determined for methanol.[33] The same anisotropic model was used for the ethers since O in both alcohols and ethers has the same sp^3 hybridization state and thus is expected to have similar shape of the polarization response. The intramolecular frame defining the polarization anisotropy was with the x-axis in the plane along the COC bisector, the y-axis is perpendicular to the COC plane, and the z-axis is orthogonal to both x and y axes. The isotropic atomic polarizability with $k_D = 1000$ kcal/(mol·Å^2) was applied to all carbon atoms.

In addition to the anisotropic polarizability, two virtual charge sites away from the atomic core were added to the ether oxygen atom to account for the asymmetry in the electron charge density around that atom. The sites are traditionally attributed to the presence of lone pairs (LPs), i.e. an electron pair in the valence shell of the atom not involved in the formation of a covalent bond. Such a model adjustment has been shown to better predict the anisotropy of the interactions of a water molecule in different orientations about hydrogen bond acceptors as compared to atom centered charges.[33,49] The determination of the LP partial charges are included in the fitting procedure. However, their positions were not optimized during the fitting but rather adjusted manually based on achieving as small as possible root-mean-square error (RMSE) of empirical vs QM electrostatic potentials (ESP) and the qualitative reproduction of the variation of the local QM ESP around the oxygen atom.[33] The CHARMM LONEPAIR facility was used for the placement of the virtual particles.

Partial atomic charges and atomic polarizabilities for the Drude polarizable model were determined from restrained fitting to the B3LYP/aug-cc-pVDZ perturbed electrostatic potential (ESP) maps using MP2/6-31G(d) optimized geometries, as previously described.[32] The ESP grid points were located on concentric nonintersecting Connolly surfaces around the ether molecule. In order to determine both atomic polarizabilities and partial atomic charges from the single fitting procedure, a series of perturbed ESP maps was generated by placing point charges of magnitude +0.5e on Connolly surfaces along chemical bonds, around the ether oxygen atoms (to probe lone pairs) and in the gaps between the initially placed ions to achieve nearly equidistant coverage of the molecular shape. Connolly surfaces of perturbation charges and grid points were generated with size factors 2.2 (charges and grid), 3.0 (grid), 4.0 (charges), 5.0 (grid), and 6.0 (grid). The size factor multiplied by the vdW radius of the corresponding atom determines its distance from the corresponding Connolly surface. In addition, for the oxygens, additional perturbation ions and grid points with a size factor of 1.3 were included. This proximal surface, along with the grid at 2.2, takes into account the details of the electrostatic environment of the molecule around the region where hydrogen-bond and other direct interactions take place, whereas the more distal surfaces provide a more accurate description of the dipolar and polarizability response of the entire molecule since the point charge approximation works well at larger distances. During fitting parabolic restraints were applied to the initial values of both the charges and polarizabilities with the weighting factor of 10^{-5} Å^{-2} for all atoms except for ether oxygens, for which 10^{-1} Å^{-2} was used in order to maintain its electroneutrality. Additionally, a flat well potential with the half-width of 0.1e was used for atomic polarizabilities. Fitting to the same charge and polarizability values was imposed for chemically equivalent atoms. For the oxygen atoms the charge was moved to LP particles during the fitting procedure, while the polarizability was maintained on the atomic core of the parent oxygen. Thus, each LP effectively receives one-half of the O charge, with the oxygen having a charge of zero. Initial values for the partial atomic charges were from the additive CHARMM model, and for atomic polarizabilities Miller's ahp polarizability values α_{ahp} were modified to account for the non-hydrogen only polarizable model being used.[32,50]

Molecular dynamics (MD) simulations were performed at 298.15 K and 1 atm pressure using the new velocity Verlet integrator[51] implemented in CHARMM. A Nosé-Hoover thermostat with a relaxation time of 0.1 ps was applied to all real atoms to control the global temperature of the system. A modified Andersen-Hoover barostat with a relaxation time of 0.1 ps was used to maintain the system at constant pressure. Condensed-phase MD simulations were performed using periodic boundary conditions and SHAKE to constrain covalent bonds involving hydrogens.[52] Electrostatic interactions were treated using particle-mesh Ewald (PME) summation[53] with a coupling parameter 0.34 and sixth-order spline for mesh interpolation. Nonbond pair lists were maintained out to 14 Å, and a real space cutoff of 12 Å was used for the electrostatic and Lennard-Jones terms with the latter truncated via an atom-based force switch algorithm,[54] unless noted. Long-range contributions to the van der Waals terms were corrected for as previously described.[55,56] The extended Lagrangian double-thermostat formalism[51] was used in all polarizable MD simulations where a mass of 0.4 amu was transferred from real atoms to the corresponding Drude particles. The amplitude of their oscillation was controlled with a separate low-temperature thermostat (at $T = 1.0$ K) to ensure that their time course approximates the SCF regimen.[51]

A box of 128 molecules was used for the pure solvent simulations of all model compounds. It was shown previously that this number of molecules is adequate to achieve convergence for Drude polarizable MD simulations of neat liquid propane to within 0.5% for both molecular volumes and heats of vaporization.[30] To obtain adequate sampling, ten independent MD simulations were run for 150 ps for the box of each model compound with different initial velocities, and the final 100 ps were used for the analysis. The results of 10 simulations were averaged to get liquid-phase properties and the standard deviations were calculated. The molecular volumes were calculated as the average volume of the monomer in the box, whereas the heats of vaporization were obtained using a difference between the average potential energy of the molecule in the gas phase and the average potential energy of the monomer in the liquid-phase plus thermal correction RT.[57] Gas-phase simulations required to calculate heats of vaporization were performed using Langevin dynamics in the SCF regimen in the case of the polarizable models. The same Drude force constants as in the condensed-phase simulations were used along with infinite nonbonded cutoffs. The friction coefficient of 5.0 ps^{-1} was applied to all real atoms. Gas-phase simulations were run individually for all 128 molecules in the respective boxes for a duration of 1000 ps with the monomer result being averaged over all 128 individual simulations. The static dielectric constants ϵ of neat liquid ethers and cycloalkanes were calculated from the dipole moment fluctuations of the box as described before.[29] The high-frequency optical dielectric constant ϵ_∞ was estimated from the Clausius-Mossotti equation, which relates ϵ_∞ to the molecular polarizability.[29,58] For additive CHARMM force field simulations ϵ_∞ was set to 1.

Free energies of aqueous solvation were obtained via free energy perturbations (FEP)[59,60] using the staged protocol developed by Deng and Roux.[61] The protocol from our previous study for calculating solvation free energy of alkanes[30] with minor modifications was utilized in this work. The solvation free energies were computed as a sum of the electrostatic, dispersive, and repulsive contributions. Each term was obtained as a difference in the free energy of the solute in water and in vacuum. The weighted histogram analysis method (WHAM)[62] was used to obtain the repulsive term of the FE, whereas thermodynamic integration (TI) was used to obtain the electrostatic and dispersive components of the free energies from the simulations. The nonbonded parameter truncation scheme applied in FEP simulations was different from that used for regular MD simulations: energy instead of force switch cutoff and no long-range LJ corrections were used since these options are currently not supported by the existing FEP code. Gas-phase simulations were performed using Langevin dynamics as described above. Separate FEP simulations consisting of 10 ps of equilibration and 50 ps of production run were performed for a given value of the coupling and/or staging parameter. Three sets of simulations with different initial structures and/or initial velocities were performed for both gas- and aqueous-phase FEP calculations from which averages and standard deviations were determined.

3. Results and Discussion

3.A. Initial Parameters and Optimization Strategy. Force field parameters were optimized to maximize the quality of the agreement with various target data while still maintaining a reasonable level of transferability. Internal parameters were initially transferred directly from CHARMM27 with additional optimization, typically to the dihedral parameters, performed as required. Electrostatic parameters were obtained, in the case of the additive model, based on reproduction of the interactions with water as well as the target condensed-phase properties. In the additive model atomic charges for all H atoms of CH_x groups were assigned to be 0.09 for consistency with the CHARMM22 and 27 force fields. The partial atomic charge of carbon atoms in CH_x groups of cycloalkanes or ethers, excluding those covalently bound to an oxygen, were adjusted to make the moiety electroneutral (i.e., -0.27 for CH_3 and -0.18 for CH_2). Atomic charges of oxygens and the adjacent carbons were determined iteratively based on the reproduction of the reference dipole moment and interactions with water. With the polarizable model, the charges and polarizabilities were obtained from the ESP fitting procedure described in the methods. The atomic polarizabilities were scaled by a factor of 0.7, consistent with that used in the SWM4-NDP water model.[28] Validation of the use of scaling was based on the reproduction of free energies of solvation as described below.

Adjustment of the Lennard-Jones parameters represents the most difficult aspect of the optimization process. Initial LJ parameters were from CHARMM27. Additional optimization was motivated by the necessity of the model to adequately reproduce the target condensed-phase properties. In addition, rare gas-model compound interactions were used as target data as developed by Yin and MacKerell.[38] In the remainder of this section the motivation for the optimization

Table 1. Pure Solvent Properties of the Alkanes Using the Modified Aliphatic LJ Parameters[a]

	experimental data[b]			C27r[c]		C27m[d]	
compound	T (K)	V_m	ΔH_{vap}	V_m	ΔH_{vap}	V_m	ΔH_{vap}
ethane	184.6	**91.8**	**3.53**	91.8 ± 0.9	3.42 ± 0.03	91.8 ± 0.8	3.42 ± 0.03
propane	231.1	**125.7**	**4.51**	126.0 ± 0.6	4.28 ± 0.03	124.7 ± 1.1	4.51 ± 0.04
butane	272.7	**160.5**	**5.37**	164.1 ± 1.3	5.05 ± 0.13	160.4 ± 0.9	5.33 ± 0.07
isobutane	261.4	**162.5**	**5.12**	162.3 ± 1.6	4.82 ± 0.06	160.5 ± 1.0	4.99 ± 0.05
heptane	298.2	**244.9**	**8.76**	248.2 ± 0.9	7.24 ± 0.16	243.4 ± 1.1	8.69 ± 0.12
	312.2	**249.1**	**8.53**	254.3 ± 1.6	6.97 ± 0.16	249.2 ± 1.5	8.45 ± 0.14
decane	298.2	**325.2**	**12.28**	327.7 ± 1.9	10.29 ± 0.22	322.4 ± 1.2	12.48 ± 0.17
	312.2	**330.0**	**12.01**	336.0 ± 1.6	9.86 ± 0.22	327.4 ± 1.7	12.27 ± 0.20

[a] Molecular volumes V_m are in Å^3; heats of vaporization ΔH_{vap} are in kcal/mol. [b] Experimental data are from ref 1. [c] CHARMM27 parameters are from ref 38 with modified alkane dihedral parameters from ref. 25. [d] C27r parameters with modified Lennard-Jones parameters from ref 30.

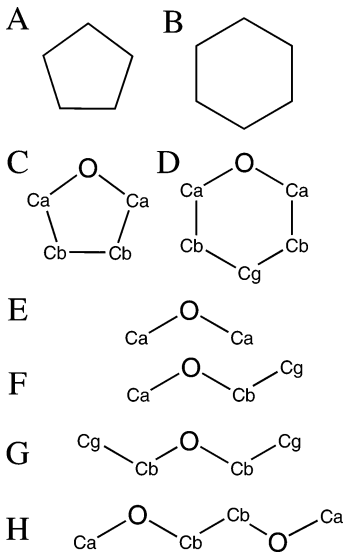

Figure 1. Model compounds: (A) cyclopentane, CPEN; (B) cyclohexane, CHEX; (C) tetrahydrofuran, THF; (D) tetrahydropyran, THP; (E) dimethyl ether, DME; (F) methyl ethyl ether MEE; (G) diethyl ether, DEE (H) 1,2-dimethoxyethane, DMOE. Atom names correspond to the atom types used in the definition of the parameters (Table S1, Supporting Information).

performed on the individual model compounds (Figure 1) is presented for the additive model followed by the polarizable one. This is followed by an overview of the results for the final selected models. Final parameters for all species are included in Table S1 of the Supporting Information.

3.B. Motivation for Selection of Final Models: Additive Force Field. As the aliphatic moieties represent a significant portion of the ethers the initial step of the parameter development was re-evaluation of the alkane parameters. This involved testing the additive linear alkanes parameters, with the LJ parameters previously developed for the Drude polarizable model, C27m,[30] along with the revised alkane dihedral parameters, C27r.[25] As may be seen in Table 1, these parameters yielded good agreement with the pure solvent properties for a range of alkanes up to decane. These parameters, which involved changes in the LJ parameters of the CH carbon and the LJ well depths of the aliphatic CH_2 hydrogens, represent a significant improvement over the original CHARMM aliphatic parameters,[38] especially in the case of the longer alkanes.

As a major goal of the present work was the development of models for cyclic ethers for use in biomolecules, tests were next undertaken to verify if the linear alkane parameters were appropriate for cyclopentane and cyclohexane. In the case of cyclohexane, good agreement was obtained for the pure solvent properties (Table 2) and for the free energies of solvation (Table 3) indicating that those parameters were acceptable. In contrast, with cyclopentane direct transfer of the alkane parameters to the five-membered ring leads to the molecular volume of 162.0 ± 1.2 Å^3 and heat of vaporization 6.39 ± 0.08 kcal/mol, which are 4.5 and −6.2% differences from experiment (Table 2), respec-

Table 2. Molecular Volumes and Heats of Vaporization for Cycloalkanes and Ethers[e]

	T, K	**exper**	additive	*%err*	Drude	*%err*
Cyclopentane (CPEN)						
V_m	298.15	**157.3**[a]	155.5 ± 0.8	*−1.2*	156.9 ± 0.9	*−0.3*
ΔH_{vap}	298.15	**6.82**[b]	6.86 ± 0.03	*0.6*	6.76 ± 0.06	*−0.9*
Cyclohexane (CHEX)						
V_m	298.15	**180.6**[b]	182.7 ± 1.0	*1.2*	182.4 ± 0.8	*1.0*
ΔH_{vap}	298.15	**7.89**[b]	7.66 ± 0.05	*−3.0*	7.67 ± 0.04	*−2.8*
Tetrahydrofuran (THF)						
V_m	298.15	**135.6**[b]	134.7 ± 0.5	*−0.7*	134.0 ± 0.8	*−1.2*
ΔH_{vap}	298.15	**7.65**[b]	7.70 ± 0.04	*0.7*	7.80 ± 0.06	*2.0*
Tetrahydropyran (THP)						
V_m	298.15	**162.3**[b]	164.3 ± 0.9	*1.2*	165.3 ± 0.3	*1.8*
ΔH_{vap}	298.15	**8.26**[b]	8.25 ± 0.07	*−0.2*	8.27 ± 0.02	*0.1*
Diethyl Ether (DEE)						
V_m	298.15	**173.9**[a]	172.4 ± 1.1	*−0.9*	171.8 ± 1.0	*−1.2*
ΔH_{vap}	298.15	**6.48**[b]	6.87 ± 0.11	*6.1*	6.80 ± 0.10	*4.9*
Dimethoxyethane (DMOE)						
V_m	298.15	**173.6**[a]	176.5 ±1.1	*1.7*	176.6 ± 0.8	*1.7*
ΔH_{vap}	298.15	**8.79**[b]	8.80 ± 0.24	*0.1*	8.79 ± 0.1	*0.0*
Dimethyl Ether (DME)						
V_m	248.34	**104.9**[c]	106.4 ± 1.1	*1.4*	106.6 ± 0.9	*1.6*
ΔH_{vap}	248.34	**5.14**[b]	5.19 ± 0.10	*0.9*	4.94 ± 0.05	*−3.9*
Methyl Ethyl Ether (MEE)						
V_m	273.20	**137.5**[d]	138.9 ± 0.9	*1.1*	137.5 ± 0.6	*−0.4*
ΔH_{vap}	280.60	**5.90**[b]	5.90 ± 0.08	*0.1*	5.72 ± 0.06	*−3.1*

[a] Experimental data are from ref 87. [b] Experimental data are from ref 1. [c] Experimental data are from ref 88. [d] Experimental data are from ref 89. [e] Molecular volumes V_m are in Å^3; heats of vaporization ΔH_{vap} are in kcal/mol.

Table 3. Solvation Free Energies in Aqueous Solution for Cycloalkanes and Ethers[a]

	exper	additive	*diff*	Drude	*diff*
CPEN	**1.20**	0.73 ± 0.21	*−0.47*	0.81 ± 0.39	*−0.39*
CHEX	**1.23**	0.89 ± 0.45	*−0.34*	1.42 ± 0.21	*0.19*
THF	**−3.47**	−3.34 ± 0.19	*0.13*	−3.78 ± 0.15	*−0.31*
THP	**−3.12**	−3.35 ± 0.05	*−0.23*	−3.20 ± 0.83	*−0.08*
DEE	**−1.76**	−2.00 ± 0.35	*−0.24*	−1.60 ± 0.11	*0.16*
DMOE	**−4.84**	−4.52 ± 0.59	*0.32*	−3.78 ± 0.59	*1.06*
DME	**−1.92**	−1.44 ± 0.32	*0.48*	−1.25 ± 0.22	*0.67*
MEE		−1.74 ± 0.22		−1.38 ± 0.16	

[a] Solvation free energies are in kcal/mol. See Table 2 and Figure 1 for compound names. Experimental data are from ref 2.

Table 4. Ether Gas-Phase Interaction Energies with a Water Molecule[a]

			QM (HF)		additive			QM (LM2/MP2)		Drude		
molec	conf	orient	**Rmin**	**IE**	Rmin	IE	*dIE*	**Rmin**	**IE**	Rmin	IE	*dIE*
THF	C2	O1_180	**2.01**	**−6.39**	1.72	−5.87	*0.52*	**1.95**	**−5.45**	1.77	−5.24	*0.20*
THF	C2	O1_120	**1.98**	**−6.95**	1.73	−6.51	*0.44*	**1.90**	**−5.95**	1.75	−5.93	*0.02*
THF	Cs	O1_180	**2.02**	**−5.99**	1.72	−6.06	*−0.07*	**1.96**	**−5.09**	1.77	−5.32	*−0.23*
THF	Cs	O1_120	**2.01**	**−6.47**	1.73	−6.47	*0.00*	**1.93**	**−5.47**	1.75	−5.80	*−0.33*
THF	***RMSE***						***0.48***					***0.32***
THP	chair	O1_180	**2.01**	**−6.05**	1.71	−6.23	*−0.18*	**1.94**	**−5.23**	*1.78*	−5.02	*0.21*
THP	chair	O1_120	**2.01**	**−6.34**	1.72	−6.49	*−0.16*	**1.92**	**−5.54**	*1.77*	−5.47	*0.08*
THP	***RMSE***						***0.17***					***0.16***
DEE	tt	O3_180	**2.03**	**−5.99**	1.75	−6.14	*−0.15*	**1.94**	**−5.41**	1.82	−5.03	*0.38*
DEE	tt	O3_120	**2.02**	**−6.76**	1.76	−6.50	*0.26*	**1.91**	**−6.00**	1.81	−5.32	*0.68*
DEE	gt	O3_180	**2.02**	**−6.16**	1.75	−5.69	*0.47*	**1.93**	**−5.60**	1.83	−4.46	*1.15*
DEE	gt	O3_120	**2.04**	**−6.47**	1.83	−6.04	*0.44*	**1.92**	**−5.99**	1.88	−4.94	*1.05*
DEE	gg	O3_180	**2.01**	**−6.21**	1.74	−5.42	*0.78*	**1.94**	**−5.49**	1.84	−4.01	*1.48*
DEE	gg	O3_120	**2.08**	**−5.88**	1.89	−5.22	*0.66*	**1.96**	**−5.44**	1.95	−4.08	*1.36*
DEE	***RMSE***						***0.51***					***1.09***
MEE	t	O3_180	**2.02**	**−5.94**	1.75	−5.69	*0.25*	**1.94**	**−5.24**	1.82	*−4.62*	*0.62*
MEE	t	O3_120	**2.02**	**−6.46**	1.76	−6.12	*0.34*	**1.92**	**−5.78**	1.81	*−5.01*	*0.78*
MEE	g	O3_180	**2.01**	**−6.09**	1.75	−5.22	*0.87*	**1.94**	**−5.56**	1.83	−4.04	*1.51*
MEE	g	O3_120	**2.04**	**−6.24**	1.83	−5.69	*0.55*	**1.94**	**−5.81**	1.88	−4.67	*1.13*
MEE	***RMSE***						***0.56***					***1.07***
DME	s	O2_180	**2.02**	**−5.87**	1.75	*−5.24*	*0.63*	**1.95**	**−5.01**	1.82	−4.23	*0.78*
DME	s	O2_180	**2.02**	**−6.10**	1.76	*−5.73*	*0.37*	**1.94**	**−5.47**	1.81	−4.71	*0.76*
DME	***RMSE***						***0.51***					***0.77***
DMOE	ttt	O2_180	**2.01**	**−5.78**	1.75	−5.32	*0.46*	**1.93**	**−5.22**	1.81	−4.48	*0.73*
DMOE	ttt	O2_120	**2.02**	**−5.95**	1.77	−5.27	*0.67*	**1.92**	**−5.42**	1.81	−4.65	*0.77*
DMOE	ttt	O2_240	**2.05**	**−5.16**	1.79	−4.71	*0.45*	**1.94**	**−5.27**	1.82	−4.36	*0.91*
DMOE	ttt	O5_180	**2.01**	**−5.78**	1.75	−5.32	*0.46*	**1.93**	**−5.22**	1.81	−4.48	*0.73*
DMOE	ttt	O5_120	**2.02**	**−5.95**	1.77	−5.27	*0.67*	**1.92**	**−5.42**	1.81	−4.65	*0.77*
DMOE	ttt	O5_240	**2.05**	**−5.16**	1.79	−4.71	*0.45*	**1.94**	**−5.27**	1.82	−4.36	*0.91*
DMOE	gtt	O2_180	**2.02**	**−5.59**	1.76	−4.80	*0.79*	**1.95**	**−5.04**	1.83	−3.92	*1.12*
DMOE	gtt	O2_120	**2.02**	**−5.83**	1.77	−5.23	*0.60*	**1.93**	**−5.19**	1.82	−4.25	*0.93*
DMOE	gtt	O2_240	**2.18**	**−3.79**	1.92	−2.98	*0.81*	**2.01**	**−4.01**	1.95	−3.22	*0.79*
DMOE	gtt	O5_180	**2.02**	**−5.38**	1.75	−4.91	*0.47*	**1.94**	**−5.04**	1.81	−4.26	*0.78*
DMOE	gtt	O5_120	**2.03**	**−5.75**	1.78	−5.10	*0.65*	**1.93**	**−5.14**	1.82	−4.44	*0.70*
DMOE	gtt	O5_240	**2.05**	**−4.86**	1.79	−4.32	*0.54*	**1.94**	**−4.93**	1.82	−4.24	*0.70*
DMOE	tgg	O2_180	**2.16**	**−4.64**	1.83	−4.66	*−0.02*	**2.03**	**−4.28**	1.86	−4.02	*0.27*
DMOE	tgg	O2_120	**2.74**	**−3.68**	2.40	−2.60	*1.08*	**2.21**	**−3.19**	1.94	−4.65	*−1.46*
DMOE	tgg	O2_240	**2.07**	**−4.57**	1.80	−4.10	*0.47*	**1.95**	**−4.81**	1.82	−4.24	*0.57*
DMOE	tgg	O5_180	**2.00**	**−6.64**	1.74	−6.31	*0.34*	**1.94**	**−5.69**	1.83	−4.51	*1.18*
DMOE	tgg	O5_120	**2.01**	**−6.39**	1.75	−6.07	*0.33*	**1.92**	**−5.57**	1.80	−4.84	*0.73*
DMOE	tgg	O5_240	**2.56**	**−5.12**	2.02	−6.10	*−0.98*	**2.29**	**−3.95**	2.40	−2.55	*1.40*
DMOE	***RMSE***						***0.62***					***0.90***

[a] Interaction energies (IE) are in kcal/mol; minimum interaction distances (Rmin) are in Å. QM data are either from scaled HF/6-31G(d)//HF/6-31G(d) (reference for additive model) or LMP2/cc-pVQZ//MP2/6-31G(d) calculations (reference for Drude model).

tively. This level of disagreement appears to be associated with strain in the smaller ring, as evidenced by increased bond lengths and the smaller angles in the 5-membered ring versus both the 6-membered ring and linear alkanes as evident from both experimental gas phase and crystal as well as QM geometric data (see Tables S2−S5 of the Supporting Information). Based on the experimental heats of vaporization a strain energy of 5.3 kcal/mol has been estimated for cyclopentane versus a negligible strain energy of −0.4 kcal/mol for cyclohexane.[63] It is therefore suggested that the strain impacts the dispersion/repulsion interactions of the molecule, requiring additional optimization of the LJ and internal parameters.

Additional support for the optimization of LJ parameters specific for cyclopentane comes from Bader's atoms in molecules theory. It was shown that the atomic properties of methyl and methylene groups in linear hydrocarbons such as charges, energies, and volumes are transferable across a series,[64,65] which is consistent with the use of the same nonbonded force field parameters. However, in cycloalkanes, due to geometric strain, differences from "standard" alkane CH_2 group atomic properties were observed for cyclopropane and to a lower degree for cyclobutane and cyclopentane. The differences in the atomic energies correlated with the experimental strain energies.[65] A noticeable increase in theatomic volume for C and decrease for H atom in cyclopropane and cyclobutane compared to average alkane values were also observed.[64] No such changes were detected for cyclohexane.[64,65] Since atomic volumes and energy might be at least qualitatively correlated to LJ radii and well depths, the requirement for unique parameters for CPEN can be thus justified.

Additional optimization of the cyclopentane LJ parameters followed the standard CHARMM procedure.[38] Following this additional optimization the resulting parameters yield excellent agreement for the pure solvent properties (Table 2) with errors well within the target values of 2%, and provided smaller fluctuations about average differences and ratios of interaction energies and distances with respect to QM data for complexes with rare gases (Table 5 and Figure 3). Moreover, the free energy of solvation is in acceptable agreement with experiment, being too favorable by ∼0.5 kcal/mol (Table 3). These LJ parameters were then used in THF during the subsequent optimization of that molecule.

Additive force field parameters were developed for the cyclic ethers, THF and THP, starting with the CH_2 group parameters for cyclopentane and cyclohexane, respectively. In the final models identical partial atomic charges and the LJ parameters of the oxygen for the two compounds were shown to reproduce interactions with water (Table 4) as well as pure solvent properties (Table 2) and the free energies of aqueous solvation (Table 3). Concerning the interactions with water, the empirical

Table 5. Root-Mean-Square Fluctuations about the Average Differences and Ratios with Respect to QM Data for the Minimum Interaction Distances and Energies for Complexes of Cycloalkanes with Helium and Neon[a]

	helium				neon			
	R_{min}		IE		R_{min}		IE	
	differ	ratio	differ	ratio	differ	ratio	differ	ratio
Cyclopentane (CPEN)								
C27r	0.0579	0.0089	17.08	0.116	0.0358	0.0101	33.64	0.0358
additive	0.0486	0.0055	16.72	0.111	0.0259	0.0065	31.76	0.0350
Drude	0.0486	0.0055	16.68	0.112	0.0259	0.0065	32.73	0.0347
Cyclohexane (CHEX)								
C27r	0.0492	0.0082	20.23	0.128	0.0249	0.0061	37.03	0.0390
additive	0.0535	0.0092	22.26	0.141	0.034	0.0089	40.28	0.0428
Drude	0.0535	0.0092	21.88	0.139	0.034	0.0089	41.84	0.0422

[a] Interaction energies (IE) are in microHartrees (mkH); minimum interaction distances (R_{min}) are in Å.

values are in good agreement with the target scaled HF/6-31G* values for the interaction energies, while the distances are underestimated by ~0.3 Å. Such an offset is consistent with previous studies showing the need for decreased minimum interaction distances in the empirical model to reproduce the density of the pure solvent.[26,27] Use of the same nonbond parameters for the oxygens indicates the transferability of the model. However, the optimized internal parameters were different reflecting the strain associated with the formation of the five-membered ring for THF, similar to that for cyclopentane.

Following completion of the cyclic ethers, the linear ethers, dimethyl ether (DME), methyl ethyl ether (MEE), diethyl ether (DEE), and dimethoxyethane (DMOE) were studied. For these compounds the oxygen LJ parameters from cyclic ethers were used directly with additional optimization of the oxygen partial atomic charges and the internal parameters undertaken. The oxygen partial charges were adjusted to better reproduce the neat liquid properties as well as interactions with water and solvation free energies across the series of compounds. In the final model the same charges were used for the oxygen and adjacent carbons in all the linear ethers. Such transferability is desirable to allow for the parameters to be applied to other ethers; however, due to simplicity of the model, it makes it impossible to reproduce all target properties with the same degree of accuracy. Thus, the final model, with a partial charge of −0.34 on the oxygens, yields good agreement for the pure solvent properties (Table 2) for all model compounds except for DEE, for which the heat of vaporization was overestimated by 6.1%. In addition, the free energy of solvation is too unfavorable by 0.5 and 0.3 kcal/mol (Table 3) for DME and DMOE, respectively, while it is slightly too favorable for DEE by 0.2 kcal/mol. These results correlate well with the interaction energies with water, which are underestimated with respect to the target data for DME, MEE, and DMOE but are in good agreement for the *tt* conformer of DEE (Table 4). Efforts to correct for the overestimation of the heat of vaporization for DEE by decreasing the partial charge on O to −0.30 lead to the reduction of this error to 2.7%. However, this DEE model underestimates the interaction energies with water (by 0.5−0.8 kcal/mol for the *tt* conformer) and solvation free energy by approximately 0.5 kcal/mol compared to target values. Moreover, the transfer of these parameters to other linear ethers leads to a substantial underestimation of the heat of vaporization (by 4.9% for DME, 3.9% for MEE and 3.0% for DMOE). Thus, the partial charge on oxygen was set to the value of −0.34 for all linear ethers in the additive model.

3.C. Motivation for Selection of Final Models: Drude Polarizable Force Field. A similar strategy as applied to the additive model was used for the development of the polarizable ether parameters. For cyclohexane direct transfer of the linear alkane charges, polarizabilities, LJ, and internal parameters lead to an underestimation of the heat of vaporization by 3.2% (not shown), while the free energy of solvation was too favorable by 0.8 kcal/mol (not shown). This motivated the refitting of the electrostatic parameters via the QM ESP approach and the scaling of the final polarizabilities by 0.7, as performed for the SWM4-NDP water model,[28] aromatic,[31] and polar-neutral species (A. D. MacKerell, Jr. et al., work in progress). This model yielded pure solvent properties in satisfactory agreement with experiment (Table 2) and, importantly, an improved free energy of solvation (Table 3). With cyclopentane, direct transfer of the linear alkane parameters again gave poor pure solvent properties (the molecular volume was too large by 5.3%, whereas the heat of vaporization was underestimated by 8.0%), and the free energy of solvation was too favorable by ca. 0.5 kcal/mol, as occurred in the additive model. Accordingly, optimized LJ and internal parameters were taken from the additive cyclopentane model, and these were initially combined with the electrostatic alkane parameters. This model did show significant improvements in the pure solvent properties (the errors in both molecular volume and heat of vaporization were less than 1%) although the free energy of solvation, as with cyclohexane, was too favorable by ~0.7 kcal/mol. Accordingly, charge and polarizability QM ESP fitting was performed with the polarizabilities scaled by 0.7, as with cyclohexane, yielding the final Drude model. This model again gave good agreement for the pure solvent properties (Table 2) and improved agreement for the free energy of solvation (Table 3), with the calculated value being ~0.4 kcal/mol more favorable than the experimental value. Thus, satisfactory polarizable models of cyclohexane and cyclopentane required explicit fitting of the charges and polarizabilities with the scaling of fitted polarizabilities by 0.7. Such scaling has been used for the aromatic and polar neutral species in the Drude model but not for the linear alkanes. The need to perform such scaling suggests that the cyclic structure of the compounds may alter their electrostatic properties, perhaps via more correlation effects due to their cyclic nature, making them behave more like polar compounds.

Initial parameters for the internal and LJ terms in the Drude polarizable model of the cyclic ethers were taken from the additive models. Partial atomic charges and atomic polarizabilities were obtained from the ESP fitting procedure, with atomic charges scaled to reproduce the reference dipole moments and the polarizabilities scaled by a factor of 0.7.

By analogy with the additive models, for THF and THP the optimized LJ parameters of the cyclopentane and cyclohexane models, respectively, were used for the C and H atoms. The LJ parameters of the oxygens were then adjusted to reproduce the pure solvent and aqueous solvation properties. The resulting models are in good agreement with experiment for both the pure solvent (Table 2) and the free energies of solvation (Table 3). The interactions energies with water are also in good agreement with the target QM data with the maximum difference being 0.3 kcal/mol (Table 4).

As with the cyclic ethers, internal parameters for the polarizable linear ethers were obtained from the additive model with the LJ parameters from the polarizable alkane force field. Charges and polarizabilities were from the ESP fitting procedure for DEE with fitted charges scaled to reproduce the experimental dipole moment and with fitted polarizabilities scaled by 0.7. These electrostatic parameters were then adjusted to produce neutral terminal CH_3 groups and then transferred to the other linear ethers, DME, MEE, and DMOE. Except for some dihedral parameters, most internal parameters were directly transferred from the corresponding additive models. To obtain a fully transferable polarizable Drude ether model and to be consistent with the additive model, oxygen LJ parameters from THF and THP models were also used for linear ethers. The resultant parameters provide reasonable agreement for both the pure solvent (Table 2) and aqueous solvation properties (Table 3). As for the additive model, the heat of vaporization of DEE is substantially overestimated (4.9%), whereas those for DME and MEE are underestimated by 3.9 and 3.1%, respectively (Table 2). However, the molecular volumes for all models were within 2% of the experimental values (Table 2). This level of agreement is similar to that of another polarizable model reported for dimethyl ether.[18] The solvation free energies are in satisfactory agreement with experiment, with the value for DEE being just 0.2 kcal/mol less favorable than the reference value, whereas those for DME and DMOE are too unfavorable by 0.7 and 1.1 kcal/mol, respectively. Such poor performance for DMOE might be related to sampling problems; additional studies are required to address this issue. It should be also noted that this linear ether model systematically underestimates the interaction energies with water, especially for DME and DMOE (Table 4), which is consistent with the trends in the solvation free energies (Table 3). Thus, the transferability of LJ parameters across ether series can be achieved, but for some compounds the agreement with experimental data needs to be sacrificed. Since the main focus of this study is the development of the ether parameters to be used in a biomolecular force field, we concentrated on the derivation of THF and THP parameters as templates for furanoses and pyranoses, respectively. The development of more accurate linear ether parameters, which are also important in biological molecules (e.g., for linkages in oligo- and polysaccharides), may require more extensive studies beyond the scope of the present work.

It should be noted that it is possible to achieve a very good agreement for a wide range of molecular properties for a particular compound. For instance, by optimizing LJ parameters of the oxygen atom we were able to obtain a Drude polarizable DEE model, which is in very good agreement for pure solvent properties (0.1% error for both molecular volume and heat of vaporization), aqueous solvation free energy (less than 0.1 kcal/mol error), and interaction energy with water (0 and 0.3 kcal/mol error for two different interaction orientations for the *tt* conformer). However, the transfer of LJ and electrostatic parameters to other linear ethers does not provide satisfactory results for condensed-phase properties: heats of vaporization are underestimated by 10.2, 8.1, and 6.8% for DME, MEE, and DMOE, respectively.

3.D. Detailed Analysis of Final Models. A variety of target data was used in the optimization of the present force field for ethers, as discussed above. In this section, the overall level of agreement with respect the various target data is presented with emphasis on the results not discussed in the preceding sections.

Gas-Phase Properties. Intramolecular parameters associated with the bond, valence angle, and dihedral angle terms in the energy function were optimized to reproduce a variety of gas-phase QM and experimental data. Presented in Tables S3−S9 of the Supporting Information is the target data along with the empirical optimized geometries for the model compounds studied. Overall the level of agreement is excellent. In virtually all cases the differences are within the target ranges of 0.02 Å, 2° and 2° for the bonds, valence angles, and dihedrals, respectively. Intramolecular parameter optimization also analyzed the vibrational spectra. As shown in Tables S10−S14 of the Supporting Information the overall level of agreement is good. Note that emphasis was placed on the treatment of the lowest frequency modes as these correspond to those that have the largest impact in MD simulations. However, for some of the lowest frequency modes, sacrifices were made in the vibrational data to allow for better reproduction of the relative energies of different conformations of the target molecules.

Table 6 lists the relative conformational energies and dipole moments of selected conformations for all model compounds. In general, the conformational energies reproduce the target MP2/cc-pVTZ//MP2/6-31G(d) data well. The energy of the planar D5h structure of cyclopentane is underestimated in the empirical models, although the energy is high enough to avoid significant sampling of this structure in MD simulations; this trend extends to THF. With cyclohexane the energies of the twist conformation are higher in the empirical models than in the QM calculations, while in THP the higher energy conformations are underestimated in the empirical models. For the cyclic ethers, the present QM data are consistent with previously reported data for THF,[67,68] including pseudorotation profiles[69−73] and THP.[74−76] Similar trends are observed in the linear alkanes with the higher energy conformations slightly overestimated in the empirical models of DEE and MEE, while they are slightly underestimated in DMOE. For DEE the experimental conformational energy difference between gt and tt is 1.14 kcal/mol in solution,[77] versus the gas-phase value of 1.36 kcal/mol, indicating potential solution effects on the conformational properties. Overall, these results along with the conformational energy surfaces shown in Figures S1−S13 of the

Table 6. Gas-Phase Relative Conformational Energies and Dipole Moments for Cycloalkanes and Ethers[a]

	relative energies			dipole moments			
	QM	additive	Drude	**exper**	**QM**	additive	Drude
Cyclopentane (CPEN)							
C2	**0.00**	0.00	0.00		**0.02**	0.05	0.02
Cs	**0.00**	0.00	0.00		**0.02**	0.05	0.02
D5h	**6.07**	4.57	3.76		**0.00**	0.00	0.00
Cyclohexane (CHEX)							
chair	**0.00**	0.00	0.00		**0.00**	0.00	0.00
twist	**6.17**	6.52	6.58		**0.00**	0.00	0.00
Tetrahydrofuran (THF)							
C2	**0.00**	0.00	0.00	**1.75**	**1.78**	1.97	1.69
Cs	**0.15**	0.30	0.15	**1.75**	**1.56**	2.12	1.78
C2v	**4.47**	3.34	2.84		**1.77**	1.99	1.70
Tetrahydropyran (THP)							
chair	**0.00**	0.00	0.00	**1.58**	**1.44**	2.03	1.58
twist25	**5.67**	5.62	5.22		**1.43**	2.03	1.61
twist14	**6.74**	6.32	6.48		**1.63**	1.98	1.67
boat25	**6.76**	6.53	6.42		**1.33**	1.98	1.62
boat14	**7.48**	7.01	6.41		**1.62**	2.05	1.64
Diethyl Ether (DEE)							
tt	**0.00**	0.00	0.00	**1.15**	**1.11**	1.81	1.20
gt	**1.36**	1.37	1.52		**1.21**	1.79	1.23
gg	**2.66**	2.94	3.24		**1.29**	1.78	1.21
Methyl Ethyl Ether (MEE)							
t	**0.00**	0.00	0.00	**1.17**	**1.19**	1.84	1.25
g	**1.38**	1.40	1.53		**1.30**	1.81	1.27
Dimethyl Ether (DME)							
s	**0.00**	0.00	0.00	**1.30**	**1.29**	1.86	1.30
Dimethoxyethane (DMOE)							
ttt	**0.00**	0.00	0.00		**0.00**	0.00	0.00
gg′t	**0.21**	0.25	0.37		**1.64**	2.04	1.45
tgt	**0.26**	0.90	0.03		**1.35**	2.30	1.67
gtt	**1.41**	1.35	1.19		**1.64**	2.37	1.66
tgg	**1.50**	2.47	1.29		**2.40**	3.64	2.46
ggg	**1.51**	3.47	2.35		**1.20**	2.66	1.86
ggg′	**1.68**	1.66	1.62		**1.91**	2.55	1.84
gtg′	**2.84**	2.48	2.41		**0.00**	0.00	0.00
gtg	**2.91**	2.63	2.30		**2.19**	3.10	2.12

[a] Relative energies are in kcal/mol; dipole moments are in Debye. Experimental data are from ref 1. QM data are from MP2/cc-pVTZ//MP2/6-31G(d) calculations.

Supporting Information support the ability of the empirical models to reproduce the target QM data.

Dipole moments of the selected conformations of the model compounds are also included in Table 6. In all cases the values for the additive model overestimate the experimental and QM target values. This is expected due to the need to implicitly overpolarize the additive model as required for treating the condensed phase due to the omission of explicit polarizability in the model.[39] With the polarizable model, the empirical values are in good agreement with the target values, a clear advantage of the polarizable model over the additive model that is anticipated to play an important role when the model is applied to environments of different polarities. There is a tendency of the polarizable model to underestimate the change in the dipole as function of conformation (e.g., THP and DMOE) although this trend is within acceptable limits.

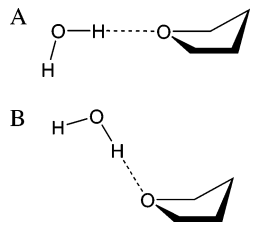

Figure 2. Interaction orientations of the C2 conformer of THF with water for the (A) orientation O1_180, where the water molecule is in the C−O1−C plane and (B) orientation O1_120 where the H atom of water molecule is oriented toward the lone pair position.

Interactions of the ethers with individual water molecules (Table 4) are worth additional discussion. Overall, the empirical values are less favorable than the target scaled HF/6-31G(d) or LMP2/cc-pVQZ(-f)//MP2/6-31G(d) QM target data for the additive and polarizable models, respectively. This is despite the additive model overestimating the dipole moments, while the polarizable models are in good agreement with the target QM and experimental data. Moreover, the condensed-phase properties are also generally in good agreement for the two empirical models. This discrepancy may be associated with the assumption in the present work that aliphatic LJ parameters are applied to the carbons adjacent to the oxygens, whereas it may be more appropriate to use "smaller" radii due to a more polar nature of these atoms. Consistent with this is the magnitude of the less favorable empirical versus QM values being smaller for the cyclic ethers relative to the linear ethers, suggesting that the constrained nature of the ring may minimize secondary interactions of the water with the surrounding aliphatic groups.

Other interesting trends in the ether−water interactions are the minimum interaction distances and the relative energies of the linear (i.e., O_180, Figure 2) and the lone pair (i.e., O_120) interactions. Overall, the empirical interaction distances are shorter than the QM values, as required to obtain the correct condensed-phase properties as previously discussed.[39] The differences are generally less in the polarizable model. This is due in part to the use of MP2 for the treatment of electron correlation in the respective target data, where the improved treatment of dispersion interactions leads to the QM minimum interaction distances being systematically shorter than the HF results. However, the minimum distances in the polarizable model are systematically longer by approximately 0.05 Å than in the additive model. Thus, the inclusion of the polarization in the force field leads to a decrease in the extent by which the empirical model must underestimate the gas phase to obtain the correct condensed-phase properties, another indication of the capability of the polarizable model to more accurately treat a wider range of environments. Concerning the relative interaction energies of the O_180 versus O_120 orientations, the empirical models typically reproduce the QM relative energies quite well. This is especially true with the polarizable model and is associated, in part, with the inclusion of virtual sites

Table 7. Dielectric Constants of Neat Liquid Cycloalkanes and Ethers[a]

molecule	*T*	**exper**	additive	*error*	Drude	*error*
CPEN	298.15	**1.96**	1.02 ± 0.00	*−0.94*	1.63 ± 0.00	*−0.33*
CHEX	298.15	**2.02**	1.02 ± 0.00	*−1.00*	1.66 ± 0.00	*−0.36*
THF	298.15	**7.43**	5.42 ± 0.33	*−2.01*	6.80 ± 0.78	*−0.63*
THP	298.15	**5.54**	4.97 ± 0.60	*−0.58*	5.03 ± 0.20	*−0.51*
DEE	298.15	**4.24**	4.96 ± 0.53	*0.72*	3.53 ± 0.34	*−0.71*
DMOE	298.15	**7.22**	6.76 ± 0.74	*−0.46*	5.61 ± 0.82	*−1.60*
DME	248.34	**6.53**	9.71 ± 1.01	3.18	6.36 ± 0.18	*−0.17*

[a] Experimental data are from ref 1.

representative of lone pairs and anisotropic polarizability on the acceptor oxygen atom.

Condensed-Phase Properties. The majority of the discussion in the preceding sections involved the condensed-phase properties, such that only issues not addressed above and additional results will be presented in this section. While the condensed-phase properties are treated in a satisfactory way in both the additive and polarizable models (Tables 2 and 3), there are discrepancies associated with the enforced use of identical parameters for the individual classes studied. Comparison of the differences with respect to experiment indicates the errors to be somewhat smaller for the additive model versus the polarizable model. For example, the average absolute percent differences for the heats of vaporization and molecular volumes are 1.1% and 1.5% for the additive model, respectively, and 1.3% and 2.2% for the polarizable model, respectively. Similarly, the average absolute differences for the free energies of solvation are 0.32 and 0.41 kcal/mol for the additive and polarizable models, respectively. While the increased discrepancies in the polarizable model are somewhat disappointing, it may possibly be attributable to the enforced transfer of the nonbond parameters. By explicitly treating polarization, the electrostatic model is suggested to be more sensitive to subtle changes in chemical structure as compared to the additive model. This additional sensitivity leads to the enforced transferability having a more negative impact in the polarizable model, leading to the poorer agreement with experiment as compared to the additive force field. Consistent with this are studies on polarizable models of the alcohols where, based on a fluctuating charge formalism, different oxygen LJ parameters were required to accurately treat methanol and ethanol,[78,79] and in a model based on a induced dipole model it was not possible to accurately reproduce the molecular volumes for the alcohol series when the same parameters were applied to the hydroxyl.[80] However, it should be reiterated that the polarizable model has the clear benefit of more accurately treating gas-phase properties as compared to the additive model while still satisfactorily treating the condensed phase, indicating the capability of the polarizable model to more accurately treat a range of condensed-phase environments from hydrophobic to highly polar.

Beyond the densities and thermodynamic properties several other properties of the ethers in the condensed phase were analyzed. Presented in Table 7 are the dielectric constants for the pure liquids. Overall the polarizable model is in better agreement with experiment, though exceptions are present. With the cyclic alkanes, the polarizable model is significantly better than the additive model, as expected as the dielectric at infinite frequency of the electric field, which is associated with the electronic polarizability of the model, dominates the total value. For the ethers, the additive model shows some significant variations from experiment, both under- and overestimating those values in the cases of THF and DME, respectively. In the polarizable model there is a systematic trend to underestimate the experimental values, with the largest discrepancy being dimethoxyethane. This trend is associated with the scaling of the polarizabilities. The use of the unscaled polarizabilities tends to increase calculated dielectric constant of both linear and cyclic ethers: e.g. DEE increases from 3.53 to 4.14, just 0.1 less than the experimental value, and THF increases from 6.80 to 8.04, which is ∼0.6 greater than the experimental estimate. However, since the remainder of the condensed-phase properties are in satisfactory agreement with experiment, the use of the scaled polarizabilities was maintained. An additional advantage of this choice is the need for such scaling in order to perform condensed-phase simulations of macromolecules. Different approaches have been used to deal with this phenomenon. For example, in the DNA simulation performed in our laboratory it was necessary to scale the polarizabilities by 0.7 to achieve a stable simulation.[32] Moreover, in an induced dipole model of proteins it was necessary to damp the polarization response between the side chains of acidic residues, Met and Tyr with TIP4Q water using a screening function,[33] while in a protein fluctuating charge model the hardness values were scaled by 1.15[81] leading to a damping of the polarization response.

One of the significant advantages of the polarizable models is the ability to more accurately treat condensed phases of different polar character as was shown previously for ion distribution near the water−air interface,[82,83] ion permeation through ion channel proteins,[84,85] and peptide folding.[86] To investigate the capability of the model to adapt to different environments, the dipole distributions were obtained for THF and diethyl ether from vacuum, aqueous solution, and pure solvent simulations. Presented in Figure 4A,B are the dipole distributions for THF and DEE for both the additive and polarizable models. For the additive model the dipole distributions are nearly identical for the gas phase, pure solvent, and aqueous solution results, with maxima in the vicinity of 2 and 1.8 Debye for THF and DEE, respectively. Such a result is expected associated with the overestimation of the dipole in the additive model and the lack of polarizability, such that the changes in the dipole moments are only due to changes in the geometry. In contrast, the differences in dipole distributions in the different environments in the polarizable model are significant. The increase in the distributions upon going from the gas to condensed phase is obvious. In the pure solvents the increase in the dipole moment versus gas phase is larger in THF than in DEE, a result consistent with the electrostatic energy contributing 13 versus 7% of the heat of vaporization in these liquids, respectively, such that the larger electrostatic contribution in THF leads to the larger increase in the dipole distribution. Upon going to aqueous solution a similar trend is observed, where the increase in the dipole distribution is

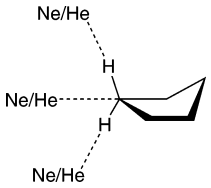

Figure 3. Interaction orientations of the C2 conformer of cyclopentane with the rare gases helium and neon. Only the hydrogens on the carbon interacting with the rare gases are shown for clarity.

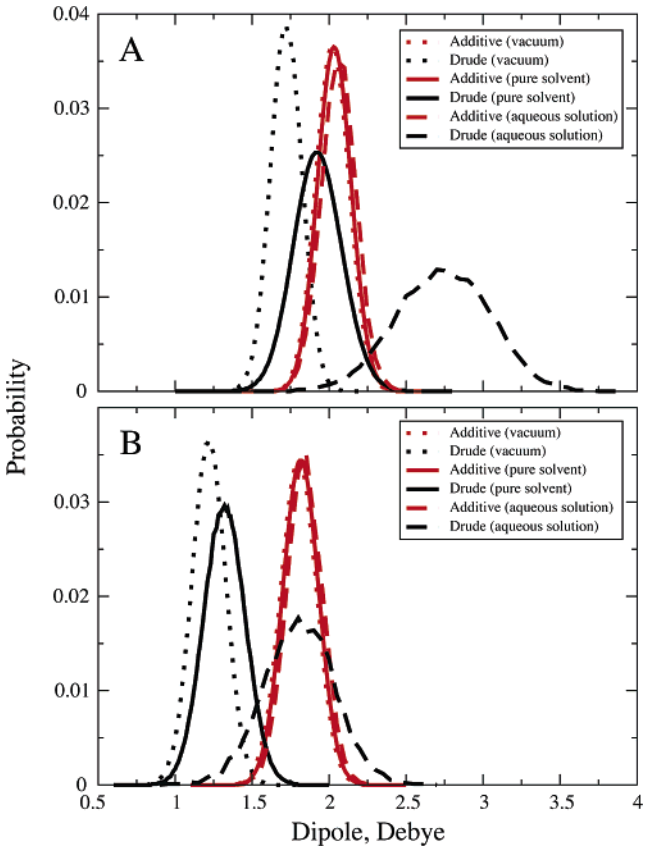

Figure 4. Dipole moment distributions for the gas, pure solvent and aqueous phases of THF (panel A) and DEE (panel B) at 298 K for both additive and Drude polarizable force fields.

larger in THF than in DEE. This is consistent with the electrostatic contribution to the free energies of solvation being −4.3 in THF and −3.2 kcal/mol in DEE, with the larger electrostatic contribution leading to the larger increase in the dipole distribution. Overall, the dipole moment in THF increases by approximately 1.1 Debye upon going from the gas phase to aqueous solution, while the corresponding value is 0.6 Debye in DEE, consistent with a greater role of electrostatics in THF.

Comparison of the additive versus polarizable dipole distributions is also interesting. As mentioned above, the additive dipole distributions are similar regardless of environment and are larger than the gas-phase values. With THF the additive distributions are slightly greater than that of the polarizable model for the pure solvent but are significantly lower than that of the polarizable dipole distribution in aqueous solution. In contrast with DEE, the additive dipole distributions are significantly higher than that of the polarizable pure solvent results, while the maxima corresponds with that of the polarizable model in aqueous solution. While the exact meaning of the differences in relative dipole distributions in the additive versus polarizable models for THF vs DEE is difficult to interpret, the observations further emphasize the utility of the polarizable models in being more responsive to the polarity of the environment as well as the inherent limitation of the additive model in treating condensed-phase properties. Last, the results indicate a more important role of electrostatics in the condensed-phase properties of THF versus DEE, consistent with the differences observed in linear versus cyclic alkanes discussed above.

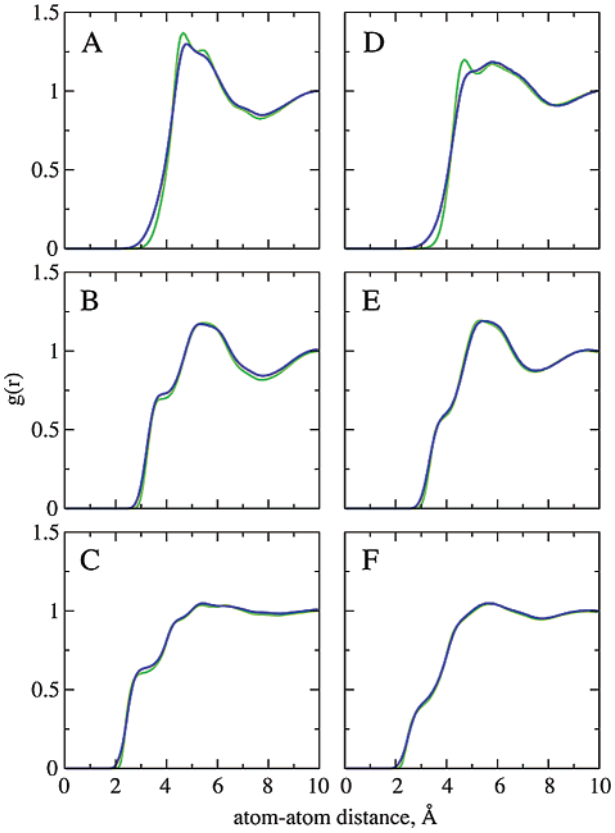

Figure 5. Radial distribution functions (RDF) for neat liquid THF (panels A−C) and DEE (panels D−F) at 298 K. O···O (A and D), C···O (B and E), and O···H (C and F) RDFs are shown for both the Drude (blue line) and additive (green line) models.

An important feature of empirical force field based calculations is that ability to obtain an atomic detail picture of condensed phases, a picture that is often difficult to obtain via experimental methods. To investigate whether the polarizable model was giving a significantly different atomic detail picture as compared to the additive models, radial distribution functions (RDF) for the THF and DEE pure solvents were analyzed. For the RDFs involving the atoms in the aliphatic moieties (i.e., C−C, C−H, and H−H RDFs) the results were very similar, though not identical, for the two models (not shown). However, RDFs involving the oxygen atom did show some differences. Presented in Figure 5 are the O−O, O−C, and O−H RDFs for both DEE and THF. In all three plots the RDF shows sampling at shorter distances in the polarizable model. This in interesting when one considers that the minimum interaction energy distances

Table 8. Pure Solvent Properties for Test Compounds[e]

	experiment	additive	%err	Drude	%err
		Molecular Volumes, Å^3			
MPE	**171.3**[a]	173.5 ± 0.7	*1.3*	172.8 ± 1.1	*0.9*
MBE	**198.0**[a]	200.1 ± 1.2	*1.1*	199.0 ± 0.7	*0.5*
EPE	**200.3**[a]	200.4 ± 0.7	*0.0*	199.6 ± 0.9	*−0.3*
MTHF	**166.7**[c]	163.0 ± 0.6	*−2.2*	162.5 ± 0.4	*−2.5*
		Heats of Vaporization, kcal/mol			
MPE	**6.60**[b]	6.70 ± 0.07	*1.6*	6.60 ± 0.12	*0.0*
MBE	**7.74**[b]	7.87 ± 0.11	*1.7*	7.75 ± 0.12	*0.1*
EPE	**7.51**[b]	7.86 ± 0.09	*4.7*	7.80 ± 0.12	*3.8*
MTHF	**8.13**[d]	8.66 ± 0.05	*6.5*	8.82 ± 0.05	*8.5*

[a] Experimental data are from ref 90. [b] Experimental data are from ref 1. [c] Experimental data are from ref 87. [d] Experimental data are from ref 91. [e] Abbreviations: MPE − methyl propyl ether, MBE − methyl butyl ether, EPE − ethyl propyl ether, MTHF − 2-methyl tetrahydrofuran.

for the interactions of water with the ether oxygens are systematically longer in the polarizable model (Table 4), suggesting that the explicit inclusion of polarizability in the model leads to "softer" interactions of the oxygen with its environment despite the use of the LJ 6-12 model to treat dispersion and exchange-repulsion in both models. Additional differences are evident in the two models at longer distances in the RDFs with the most obvious occurring in the O...O RDF. In the additive model there is a well-defined peak at 4.6 Å followed by a second peak at 5.5 Å. In contrast, the polarizable model has a broader, single peak with the maximum at 4.8 Å followed the broad peak with evidence of a small depression in the peak at 5.2 Å. Thus, the polarizable model is giving a different atomic detail picture as compared to the additive model in addition to differences in the dipole distributions and other properties discussed above.

3.E. Validation of the Developed Force Field. To validate the developed ether force field pure solvent calculations were performed on additional model compounds, including longer chain linear ethers (methyl propyl ether, methyl butyl ether, and ethyl propyl ether) and 2-methyl THF. The results are presented in Table 8. For the new compounds, the molecular volumes and most heats of vaporization are in satisfactory agreement with experimental values. For the linear ethers the largest differences are in the heats of vaporization of ethyl propyl ether which are overestimated by 4.7 and 3.8% in the additive and the Drude models, respectively, similar to the overestimation observed for DEE (Table 2). With the only cyclic test molecule, the molecular volumes are somewhat underestimated, and the heats of vaporization are overestimated with both force fields. The significant overestimation of the heat of vaporization may be associated with the addition of a methyl group on the carbon adjacent to the ether oxygen. While the origins and possible solution of these differences are beyond the scope of the present work, the overall quality of the agreement with experiment for the test molecules demonstrates the transferability of the developed LJ and electrostatic parameters.

4. Conclusion

Presented are both additive and polarizable force fields for linear and cyclic ethers. The initial stage of the optimization was the evaluation of the linear alkane parameters in cycloalkanes. While the linear alkane parameters transferred well to cyclohexane, they were not appropriate for cyclopentane. This is indicated to be due to strain in the smaller ring leading to the need for alternative LJ parameters for that model. In addition, for the polarizable model it was observed that the charges and polarizabilities from the linear alkanes were not appropriate for both cycloalkanes, requiring explicit determination of the electrostatic parameters via the QM fitting procedure followed by scaling of the polarizabilities by 0.7. These steps are suggested to be due to the cyclic alkanes having a more polar character due to more correlated electronic effects associated with their cyclic structures.

The alkane parameters were then used directly in the ethers, with the new cyclopentane based parameters used in THF, with the only LJ parameters optimized being those of oxygen. In the additive models, the charges on the oxygen, with appropriate adjustments of the adjacent carbons, were optimized based on interactions with water, while the charges were determined via the QM ESP approach for the polarizable model. Selected internal parameters, primarily associated with dihedrals, were optimized as required. To facilitate the transferability of the parameters, the LJ parameters and electrostatic parameters for all the linear ethers were constrained to be identical for the respective electrostatic models. However, due to the ring strain discussed above, the electrostatic parameters of THF were allowed to differ from THP, although in the additive model the same charge was found to be appropriate for both compounds. Further, the LJ parameters of the oxygens were identical for all ethers of a given electrostatic model.

Optimization of the parameters based on the above restraints yielded models that are in satisfactory agreement with both pure solvent properties and free energies of aqueous solvation. As is typical for additive models, this was achieved via implicit overpolarization of the charge distribution such that the gas-phase dipole moments and interactions with water were overestimated. In contrast, the polarizable model allowed both gas phase and condensed-phase properties to be reproduced reasonably well. This represents a major advantage of the polarizable model that should allow it to more accurately treat ethers in a wider variety of environments ranging from hydrophobic to aqueous solution. This is emphasized by the changes in the dipole distribution of THF and DEE in MD simulations of the gas phase, in aqueous solution, and in the pure solvents. In addition, RDFs show that differences in the atomic interactions, especially those involving the oxygens, occur in the polarizable versus additive models.

Somewhat disappointing is the inability of the polarizable model to yield overall improvements in condensed-phase properties as compared to the additive model. Given the extra degrees of freedom in the polarizable model it would be assumed that improved agreement should be achieved. The reason this was not achieved is suggested to be due to the restraints in the parametrization enforced to facilitate trans-

ferability. Due to the polarizable electrostatic model being more sensitive to the environment, including intramolecular contributions, the use of the restraints in the parameters appears to have a larger negative impact than in the additive model, where the electrostatic properties are not affected by the environment. Future studies will address this issue.

Acknowledgment. Financial support from the NIH (GM51501 and GM72558) is acknowledged, and the DOD ACS Major Shared Resource Computing and PSC Pittsburgh Supercomputing Center are thanked for their generous CPU allocations.

Supporting Information Available: Optimized force field parameters; experimental, QM and CHARMM calculated molecular geometries, and vibrational frequencies; QM and force field based torsional energy profiles. This material is available free of charge via the Internet at http://pubs.acs.org.

References

(1) *CRC Handbook Chemistry and Physics*, 84th ed.; Lide, D. R., Ed.; CRC Press: Boca Raton, 2003; p 2616.

(2) Kelly, C. P.; Cramer, C. J.; Truhlar, D. G. *J. Chem. Theory Comput.* **2005**, *1*, 1133.

(3) Halgren, T. A. *J. Comput. Chem.* **1996**, *17*, 490.

(4) Allinger, N. L.; Chen, K. H.; Lii, J. H.; Durkin, K. A. *J. Comput. Chem.* **2003**, *24*, 1447.

(5) Lii, J. H.; Chen, K. H.; Allinger, N. L. *J. Phys. Chem. A* **2004**, *108*, 3006.

(6) Lii, J. H.; Chen, K. H.; Allinger, N. L. *J. Comput. Chem.* **2003**, *24*, 1504.

(7) Lii, J. H.; Chen, K. H.; Durkin, K. A.; Allinger, N. L. *J. Comput. Chem.* **2003**, *24*, 1473.

(8) Lii, J. H.; Chen, K. H.; Grindley, T. B.; Allinger, N. L. *J. Comput. Chem.* **2003**, *24*, 1490.

(9) Briggs, J. M.; Matsui, T.; Jorgensen, W. L. *J. Comput. Chem.* **1990**, *11*, 958.

(10) Jorgensen, W. L.; Maxwell, D. S.; Tirado-Rives, J. *J. Am. Chem. Soc.* **1996**, *118*, 11225.

(11) Helfrich, J.; Hentschke, R. *Macromolecules* **1995**, *28*, 3831.

(12) Girard, S.; Muller-Plathe, F. *Mol. Phys.* **2003**, *101*, 779.

(13) Faller, R.; Schmitz, H.; Biermann, O.; Muller-Plathe, F. *J. Comput. Chem.* **1999**, *20*, 1009.

(14) Cornell, W. D.; Cieplak, P.; Bayly, C. I.; Gould, I. R.; Merz, K. M.; Ferguson, D. M.; Spellmeyer, D. C.; Fox, T.; Caldwell, J. W.; Kollman, P. A. *J. Am. Chem. Soc.* **1995**, *117*, 5179.

(15) Weiner, S. J.; Kollman, P. A.; Case, D. A.; Singh, U. C.; Ghio, C.; Alagona, G.; Profeta, S.; Weiner, P. *J. Am. Chem. Soc.* **1984**, *106*, 765.

(16) Weiner, S. J.; Kollman, P. A.; Nguyen, D. T.; Case, D. A. *J. Comput. Chem.* **1986**, *7*, 230.

(17) Borodin, O.; Smith, G. D. *J. Phys. Chem. B* **2003**, *107*, 6801.

(18) Borodin, O.; Smith, G. D. *J. Phys. Chem. B* **2006**, *110*, 6279.

(19) Bedrov, D.; Smith, G. D. *J. Phys. Chem. B* **1999**, *103*, 10001.

(20) Bedrov, D.; Smith, G. D. *J. Phys. Chem. B* **1999**, *103*, 3791.

(21) Bedrov, D.; Pekny, M.; Smith, G. D. *J. Phys. Chem. B* **1998**, *102*, 996.

(22) Bedrov, D.; Borodin, O.; Smith, G. D. *J. Phys. Chem. B* **1998**, *102*, 5683.

(23) Bedrov, D.; Borodin, O.; Smith, G. D. *J. Phys. Chem. B* **1998**, *102*, 9565.

(24) Foloppe, N.; MacKerell, A. D., Jr. *J. Comput. Chem.* **2000**, *21*, 86.

(25) Klauda, J. B.; Brooks, B. R.; MacKerell, A. D., Jr.; Venable, R. M.; Pastor, R. W. *J. Phys. Chem. B* **2005**, *109*, 5300.

(26) MacKerell, A. D., Jr.; Wiyrkiewicz-Kuczera, J.; Karplus, M. *J. Am. Chem. Soc.* **1995**, *117*, 11946.

(27) MacKerell, A. D., Jr.; Bashford, D.; Bellott, M.; Dunbrack Jr., R. L.; Evanseck, J.; Field, M. J.; Fischer, S.; Gao, J.; Guo, H.; Ha, S.; Joseph, D.; Kuchnir, L.; Kuczera, K.; Lau, F. T. K.; Mattos, C.; Michnick, S.; Ngo, T.; Nguyen, D. T.; Prodhom, B.; Reiher, I., W. E.; Roux, B.; Schlenkrich, M.; Smith, J.; Stote, R.; Straub, J.; Watanabe, M.; Wiorkiewicz-Kuczera, J.; Yin, D.; Karplus, M. *J. Phys. Chem. B* **1998**, *102*, 3586.

(28) Lamoureux, G.; Harder, E.; Vorobyov, I. V.; Roux, B.; MacKerell, A. D., Jr. *Chem. Phys. Lett.* **2006**, *418*, 245.

(29) Lamoureux, G.; MacKerell, A. D., Jr.; Roux, B. *J. Chem. Phys.* **2003**, *119*, 5185.

(30) Vorobyov, I. V.; Anisimov, V. M.; MacKerell, A. D., Jr. *J. Phys. Chem. B* **2005**, *109*, 18988.

(31) Lopes, P. E. M.; Lamoureux, G.; Roux, B.; MacKerell, A. D., Jr. *J. Chem. Theory Comput.* **2007**, *3*, in press.

(32) Anisimov, V. M.; Lamoureux, G.; Vorobyov, I. V.; Huang, N.; Roux, B.; MacKerell, A. D., Jr. *J. Chem. Theory Comput.* **2005**, *1*, 153.

(33) Harder, E.; Anisimov, V. M.; Vorobyov, I. V.; Lopes, P. E. M.; Noskov, S. Y.; MacKerell, A. D., Jr.; Roux, B. *J. Chem. Theory Comput.* **2006**, *2*, 1587.

(34) Frisch, M. J.; Trucks, G. W.; Robb, M. A.; Scuseria, G. E.; Schlegel, H. B.; Cheeseman, J. R.; Montgomery, J. J. A.; Vreven, T.; Kudin, K. N.; Burant, J. C.; Millam, J. M.; Iyengar, S. S.; Tomasi, J.; Barone, V.; Mennucci, B.; Cossi, M.; Scalmani, G.; Rega, N.; Petersson, G. A.; Nakatsuji, H.; Hada, M.; Ehara, M.; Toyota, K.; Fukuda, R.; Hasegawa, J.; Ishida, M.; Nakajima, T.; Honda, Y.; Kitao, O.; Nakai, H.; Klene, M.; Li, X.; Knox, J. E.; Hratchian, H. P.; Cross, J. B.; Bakken, V.; Adamo, C.; Jaramillo, J.; Gomperts, R.; Stratmann, R. E.; Yazyev, O.; Austin, A. J.; Cammi, R.; Pomelli, C.; Ochterski, J. W.; Ayala, P. Y.; Morokuma, K.; Voth, G. A.; Salvador, P.; Dannenberg, J. J.; Zakrzewski, V. G.; Dapprich, S.; Daniels, A. D.; Strain, M. C.; Farkas, O.; Malick, D. K.; Rabuck, A. D.; Raghavachari, K.; Foresman, J. B.; Ortiz, J. V.; Cui, Q.; Baboul, A. G.; Clifford, S.; Cioslowski, J.; Stefanov, B. B.; Liu, G.; Liashenko, A.; Piskorz, P.; Komaromi, I.; Martin, R. L.; Fox, D. J.; Keith, T.; Al-Laham, M. A.; Peng, C. Y.; Nanayakkara, A.; Challacombe, M.; Gill, P. M. W.; Johnson, B.; Chen, W.; Wong, M. W.; Gonzalez, C.; Pople, J. A. *Gaussian 03, Revision C.02*; Gaussian, Inc.: Wallingford, CT, 2004.

(35) Foloppe, N.; Nilsson, L.; MacKerell, A. D., Jr. *Biopolymers (Nucleic Acid Sciences)* **2002**, *61*, 61.

(36) Greene, S.; Guvench, O.; MacKerell, A. D., Jr. unpublished data, 2006.

(37) Woodcock, H. L.; Moran, D.; Pastor, R. W.; MacKerell, A. D., Jr.; Brooks, B. R. *Biophys. J.*, in press.

(38) Yin, D.; MacKerell, A. D., Jr. *J. Comput. Chem.* **1998**, *19*, 334.

(39) MacKerell, A. D., Jr. *J. Comput. Chem.* **2004**, *25*, 1584.

(40) *Jaguar*, 4.2 ed.; Schrodinger, Inc.: Portland, OR, 2000.

(41) Huang, N.; MacKerell, A. D., Jr. *J. Phys. Chem. B* **2002**, *106*, 7820.

(42) Saebo, S.; Pulay, P. *Annu. Rev. Phys. Chem.* **1993**, *44*, 213.

(43) Saebo, S.; Tong, W.; Pulay, P. *J. Chem. Phys.* **1993**, *98*, 2170.

(44) Allen, F. H. *Acta Crystallogr. B* **2002**, *58*, 380.

(45) CCDC. *Vista - A Program for the Analysis and Display of Data Retrieved from the CSD*; Cambridge Crystallographic Data Centre: Cambridge, England, 1994.

(46) MacKerell, A. D.; Jr.; Brooks, B.; Brooks, C. L., III; Nilsson, L.; Roux, B.; Won, Y.; Karplus, M. CHARMM: The Energy Function and Its Paramerization with an Overview of the Program. In *Encyclopedia of Computational Chemistry*; Schleyer, P. v. R., Allinger, N. L., Clark, T., Gasteiger, J., Kollman, P. A., Schaefer, H. F., III, Schreiner, P. R., Eds.; John Wiley & Sons: Chichester, 1998; Vol. 1, p 271.

(47) Brooks, B. R.; Bruccoleri, R. E.; Olafson, B. D.; States, D. J.; Swaminathan, S.; Karplus, M. *J. Comput. Chem.* **1983**, *4*, 187.

(48) Thole, B. T. *Chem. Phys.* **1981**, *59*, 341.

(49) Dixon, R. W.; Kollman, P. S. *J. Comput. Chem.* **1997**, *18*, 1632.

(50) Miller, K. J. *J. Am. Chem. Soc.* **1990**, *112*, 8533.

(51) Lamoureux, G.; Roux, B. *J. Chem. Phys.* **2003**, *119*, 3025.

(52) Ryckaert, J. P.; Ciccotti, G.; Berendsen, H. J. C. *J. Comput. Phys.* **1977**, *23*, 327.

(53) Darden, T.; York, D.; Pedersen, L. *J. Chem. Phys.* **1993**, *98*, 10089.

(54) Steinbach, P. J.; Brooks, B. R. *J. Comput. Chem.* **1994**, *15*, 667.

(55) Allen, M. P.; Tildesley, D. J. *Computer Simulation of Liquids*; Clarendon Press: Oxford, 1987; p 408.

(56) Lague, P.; Pastor, R. W.; Brooks, B. R. *J. Phys. Chem. B* **2004**, *108*, 363.

(57) Ben-Naim, A. *Statistical Thermodynamics for Chemists and Biochemists*; Plenum Press: New York, 1992; p 720.

(58) Bonin, K. D.; Kresin, V. V. *Electric-dipole polarizabilities of atoms, molecules, and clusters*; World Scientific: Singapore River Edge, NJ, 1997; p 247.

(59) Kollman, P. A. *Chem. Rev.* **1993**, *93*, 2395.

(60) Simonson, T. Free Energy Calculations. In *Computational Biochemistry and Biophysics*; Becker, O. M., MacKerell, A. D., Jr., Roux, B., Watanabe, M., Eds.; Marcel Dekker, Inc.: New York, 2001; p 169.

(61) Deng, Y.; Roux, B. *J. Phys. Chem. B* **2004**, *108*, 16567.

(62) Kumar, S.; Bouzida, D.; Swendsen, R. H.; Kollman, P. A.; Rosenberg, J. M. *J. Comput. Chem.* **1992**, *13*, 1011.

(63) Boatz, J. A.; Gordon, M. S.; Hilderbrandt, R. L. *J. Am. Chem. Soc.* **1988**, *110*, 352.

(64) Bader, R. F. W.; Carroll, M. T.; Cheeseman, J. R.; Chang, C. *J. Am. Chem. Soc.* **1987**, *109*, 7968.

(65) Wiberg, K. B.; Bader, R. F. W.; Lau, C. D. H. *J. Am. Chem. Soc.* **1987**, *109*, 1001.

(66) Borodin, O.; Smith, G. D. *J. Phys. Chem. B* **2006**, *110*, 6293.

(67) Strajbl, M.; Florian, J. *Theor. Chem. Acc.* **1998**, *99*, 166.

(68) Strajbl, M.; Baumruk, V.; Florian, J. *J. Phys. Chem. B* **1998**, *102*, 1314.

(69) Rayon, V. M.; Sordo, J. A. *J. Chem. Phys.* **2005**, *122*, 204303.

(70) Gallinella, E.; Cadioli, B.; Flament, J. P.; Berthier, G. *J. Mol. Struct.* (*Theochem*) **1994**, *121*, 137.

(71) Cadioli, B.; Gallinella, E.; Coulombeau, C.; Jobic, H.; Berthier, G. *J. Phys. Chem.* **1993**, *97*, 7844.

(72) Berthier, G.; Cadioli, B.; Gallinella, E.; Aamouche, A.; Ghomi, M. *J. Mol. Struct.* (*Theochem*) **1997**, *390*, 11.

(73) Berthier, G.; Cadioli, B.; Gallinella, E. *Theor. Chem. Acc.* **2000**, *104*, 223.

(74) Freeman, F.; Kasner, M. L.; Hehre, W. J. *J. Phys. Chem. A* **2001**, *105*, 10123.

(75) Freeman, F.; Kasner, J. A.; Kasner, M. L.; Hehre, W. J. *J. Mol. Struct. (Theochem)* **2000**, *496*, 19.

(76) Ionescu, A. R.; Berces, A.; Zgierski, M. Z.; Whitfield, D. M.; Nukada, T. *J. Phys. Chem. A* **2005**, *109*, 8096.

(77) Halgren, T. A. *J. Comput. Chem.* **1999**, *20*, 730.

(78) Patel, S.; Brooks, C. L. *J. Chem. Phys.* **2005**, *122*, 024508.

(79) Patel, S.; Brooks, C. L. *J. Chem. Phys.* **2005**, *123*, 164502.

(80) Gao, J. L.; Habibollazadeh, D.; Shao, L. *J. Phys. Chem.* **1995**, *99*, 16460.

(81) Patel, S.; Brooks, C. L., III. *J. Comput. Chem.* **2004**, *25*, 1.

(82) Archontis, G.; Leontidis, E.; Andreou, G. *J. Phys. Chem. B* **2005**, *109*, 17957.

(83) Jungwirth, P.; Tobias, D. J. *Chem. Rev.* **2006**, *106*, 1259.

(84) Allen, T. W.; Andersen, O. S.; Roux, B. *Proc. Natl. Acad. Sci. U.S.A.* **2004**, *101*, 117.

(85) Allen, T. W.; Andersen, O. S.; Roux, B. *Biophys. Chem.* **2006**, *124*, 251.

(86) Soto, P.; Mark, A. E. *J. Phys. Chem. B* **2002**, *106*, 12830.

(87) Poling, B. E.; Prausnitz, J. M.; O'Connell, J. P. *The properties of gases and liquids*, 5th ed.; McGraw-Hill: New York, 2001; p 752.

(88) Wu, J. T.; Liu, Z. G.; Bi, S. S.; Meng, X. Y. *J. Chem. Eng. Data* **2003**, *48*, 426.

(89) Liu, Z. Y.; Chen, Z. C. *Chem. Eng. J. Bioch. Eng.* **1995**, *59*, 127.

(90) Obama, M.; Oodera, Y. *J. Chem. Eng. Data* **1985**, *30*, 1.

(91) Chicos, J. S.; Acree, W. E., Jr. *J. Phys. Chem. Ref. Data* **2003**, *32*, 519.

CT600350S